J Therm Anal Calorim (2012) 108:799–806
DOI 10.1007/s10973-011-2083-7

Kinetic evaluation of non-isothermal crystallization of oxidized extra virgin olive oil

Emma Chiavaro · Lorenzo Cerretani · Maria Paciulli · Stefano Vecchio

MEDICTA2011 Conference Special Chapter

Abstract In this study, accelerated storage tests were carried out at 60 °C up to 20 weeks on three extra virgin olive oils (Evoos) with different total phenol contents and fatty acid compositions (named as EvooA, EvooB, and EvooC). Their oxidative statuses, evaluated by means of primary oxidation value and total phenolic content, were related to both the shapes of differential scanning calorimetry (DSC) cooling curves and thermal properties. DSC cooling curves were all deconvoluted as crystallization occurs in a quite narrow range, and the single steps are not well separated. The first deconvoluted DSC peak for the three samples tested, which occurs in the temperature interval between −45 °C and −30 °C, can probably be ascribable to the crystallization of tri-unsaturated triacylglycerols. A non-isothermal crystallization kinetic procedure, derived by the well-known isothermal Avrami equation, combined with the method of Ozawa, was applied to the first deconvoluted DSC peak only by processing the data related to this DSC peak. Results of the modified Avrami method were found in agreement with those of the Ozawa method. In particular, Avrami and Ozawa's exponents lie from 2 to 4 (being those of fresh samples always lower than those subjected to the accelerated oxidation test). Crystallization is relatively slow for fresh samples whereas after the first 4 weeks; it occurs faster in EvooB and EvooC.

Keywords Extra virgin olive oil · Differential scanning calorimetry · Non-isothermal crystallization kinetics · Ozawa-Avrami method

E. Chiavaro · M. Paciulli
Dipartimento di Ingegneria Industriale, Università degli Studi di Parma, Parco Area delle Scienze 181/A, I-43124 Parma, Italy

L. Cerretani
Dipartimento di Economia e Ingegneria Agrarie, Università di Bologna, p.zza Goidanich 60, I-47521 Cesena, FC, Italy

S. Vecchio (✉)
Dipartimento di Scienze di Base e Applicate all'Ingegneria, via del Castro Laurenziano 7, I-00185 Rome, Italy
e-mail: stefano.vecchio@uniroma1.it

Introduction

Extra virgin olive oil (Evoo) is obtained by the fruit of the olive tree solely by mechanical or other physical means that do not lead to any chemical change. It presents a high resistance to the oxidative deterioration due not only to the high monounsaturated-to polyunsaturated fatty acid ratio but also to the presence of such minor compounds as phenolic molecules with antioxidant activity, with almost all of them being hydrophilic [1].

Evoo is generally consumed raw as a flavoring fat at room temperature. Otherwise, it can be employed as lipid phase and/or filling medium in a wide range of food formulations, such as canned products, salad dressings, sauces, and chilled and frozen ready-to-eat commodities. All these products could be stored for long time, before being consumed, at refrigerated and frozen temperatures where lipids begin to crystallize also starting from a different degree of oxidation. In addition, Evoo crystallization could become more complex due to its high content of water (it is directly obtained by fruit physical extraction without further refining), which is organized to form small dispersed particles with hydrophilic phenols being located on their surface at the oil–water interface [2]. The influence of these molecules on Evoo stability during crystallization was recently demonstrated [3]. Their decrement in the liquid phase surrounding fat crystals can concur with the higher

oxidation rate shown by this oil (on the basis of the Arrhenius equation) at sub-zero temperatures [3].

Non-isothermal crystallization kinetics was analyzed in the past using different methods for the characterization of a wide variety of amorphous systems (i.e., paraffins [4], glass [5–7], and polymers [8–12]), but less attention was devoted to this approach applied to food matrices and oil, among all [3, 13]. This study aims at analyzing the influence of the oxidation stage in the non-isothermal crystallization kinetics of three Evoo samples (having different total phenol contents and fatty acid compositions). To this end, fresh samples and samples subjected to an accelerated storage test at 60 °C for 4, 12, and 20 weeks were considered. This temperature was chosen as it is generally considered as the one that mimics oxidation mechanism developing during normal storage in a better way [1].

Theoretical background

Isothermal crystallization rate is usually described by the Avrami equation [14, 15], whose general form is:

$$1 - X(t) = \exp(-Kt^n) \quad (1)$$

where $X(t)$, the degree of crystallinity, is the ratio between the partial and the total heats released measured by numerical integration of the areas of the corresponding crystallization DSC peak. Deconvolution of the DSC peak into two or more peaks is required if crystallization occurs in several simultaneous steps to estimate the area of each peak, associated to each step. K and n, characteristic constants of a particular morphology and type of nucleation, are the crystallization rate constant and the Avrami index, respectively, and t is the time taken during the crystallization process. The value of the Avrami index n, related to both nucleation and growth geometry, should be an integer, but several complications that often arise due to volume changes for the occurrence of a phase transformation, annealing, and different mechanisms involved during the process or incomplete crystallization, may give rise to fractional values.

The isothermal Avrami approach can be adjusted to non-isothermal condition by considering the double logarithmic form of Eq. 1, where the values of n and K can be estimated at each fixed temperature, from the slope and intercept of each $\ln\{-\ln[1-X(t)]\}$ versus $\ln(t)$ straight line, where $t = (T_0-T)/\beta$.,with β being the cooling rate, T_0 and T the onset crystallization temperature and the crystallization temperature at time t, respectively. A further correction was introduced by Jeziorny [16] to calculate more reliable values of K from non-isothermal measurements since crystallization depends on the cooling rate: $\ln K' = (\ln K)/\beta$.

Taking into account the non-isothermal nature of a crystallization process, Ozawa [17] modified the Avrami equation by assuming that a non-isothermal process is the sum of an infinite number of small isothermal steps, according to the following logarithmic Eq. 2:

$$-\ln[1 - X(t)] = K^*(T)/\beta^m \quad (2)$$

where $K^*(T)$, the cooling crystallization temperature-dependent function, is referred to the overall crystallization rate (indicating how fast this process occurs [18]) and m is the Ozawa exponent that depends on the dimension of the crystal growth. Eq. 2 can be more conveniently rewritten in the logarithmic form (Eq. 3):

$$\ln\{-\ln[1 - X(t)]\} = \ln(K^*(T)) - m\ln\beta \quad (3)$$

By plotting the left-hand side of Eq. 3 versus $\ln\beta$, a straight line chould be obtained, where the $K^*(T)$ and m values can be obtained from the intercept and slope of the corresponding regression line (least square method), respectively.

Liu and co-workers [19] proposed to combine the Avrami and Ozawa approaches by making the double logarithmic form of Eq. 1 equal to the right-hand side of Eq. 3:

$$\ln K + n\ln t = \ln(K^*(T)) - m\ln\beta \quad (4)$$

that can be rewritten in the form:

$$\ln\beta = \ln F(T) - b\ln t \quad (5)$$

where $F(T) = [K^*(T)/K]^{1/m}$ refers to a given cooling rate and to a fixed degree of crystallinity, m is calculated using the method of Ozawa, and b is the ratio between the exponents of Avrami and Ozawa, respectively.

Experimental

Samples and storage conditions

The Evoo samples tested in this study, and selected considering three estimated levels of total phenol contents (high, medium, and low, respectively), were obtained from olives handpicked in 2009 and produced using continuous cold extraction systems. In particular, sample A (EvooA) is a blend of Leccino, Frantoio, Moraiolo, and local varieties, derived from Emilia Romagna; sample B (EvooB) from Apulia (blend of Ogliarola di Lecce and Cellina di Nardò varieties), and sample C (EvooC) from Emilia Romagna (blend of Frantoio, Leccino, Pendolino and Moraiolo varieties).

Each sample was divided into four aliquots (43.7 mL, 40 g) and kept in the dark at 60 °C in a thermostatic oven (ISCO, Milano, Italy) for 20 weeks. Each aliquot was

stored in an individual open glass bottle of 250 mL (i.d. = 5 cm; surface area exposed to air 19.6 cm^2). Bottles were removed from the oven after 4, 12, and 20 weeks, and immediately analyzed.

Chemical analysis

Fatty acids were determined on fresh samples according to Bendini et al. [20] methyl esters by capillary gas chromatography (GC) analysis after alkaline treatment and expressed as area normalization in percent (%). Total phenol contents were obtained on fresh samples by means of spectrophotometric assay according to Bonoli et al. [21] and expressed as mg gallic acid/kg oil.

Oxidation degree was measured by means of peroxide value (POV, expressed as meq O_2/kg lipids) according to the official methods described in annex III of EEC Regulation 2568/91 [22] on fresh samples and after 4, 12, and 20 weeks of storage. Three replicates were analysed per sample.

DSC experiments

Evoo samples, around 8–10 mg, were weighed in aluminum pans; covers were sealed into place and analyzed with a DSC Q100 (TA Instruments, New Castle, DE, USA), and an empty pan was used as reference. Calibrations of both heat flow and temperature were made using very pure samples of indium (T_{fus} = 156.6 °C, $\Delta_{fus}H$ = 3.266 kJ mol^{-1}) and *n*-dodecane (T_{fus} = −9.65 °C, $\Delta_{fus}H$ = 36.918 J mol^{-1}). The temperature and heat flow uncertainties were estimated to be ±0.1 °C and ±0.05 mW, respectively. DSC cooling curves were obtained at four scanning rates (1, 2, 3, and 5 °C min^{-1}) keeping oils at 30 °C for 8 min to reach equilibrium and then cooling up to −80 °C. Dry nitrogen was purged in the DSC apparatus at a flow rate of 50 cm^3 min^{-1}. Three replicates were analyzed per sample.

DSC cooling curves were analyzed with Universal Analysis Software (Version 3.9A, TA Instruments), converted in ASCII compatible format and best deconvoluted by means of PeakFitTM software (Jandel Scientific, San Rafael, CA, USA) into three constituent peaks ($R^2 \geq 0.98$), as previously reported [23]. The three peaks identified were consecutively numbered, starting from the lowest to the highest temperature and named as peaks 1, 2, and 3, respectively. Peak 1 was resolved by an asymmetric double Gaussian, while peaks 2 and 3 by double sigmoid functions [23]. Deconvoluted DSC curves were re-imported in Universal Analysis Software where area of peak 1, which was the only one considered for the crystallization evaluation, was calculated with the integration function of software and converted in ASCII compatible format again to obtain fraction of peak area at each time interval.

Results and discussion

Chemical analysis

The three Evoo samples of this study were chosen on the basis of different fatty acid compositions and phenol contents. EvooA exhibited significantly high percentages of oleic acid (74%) and the lowest content of linoleic acid (6.2%) among all. On the other hand, EvooB presented the lowest content in oleic acid (65%) and the highest in palmitic (15.4%) and linoleic (10.0%) acids, whereas EvooC showed a middle fatty acid composition between EvooA and EvooB (71.6 and 8.1% of oleic and linoleic acid amounts, respectively). These compositional data are completed by the differences in total phenol amount as EvooA showed high content of total phenolic compounds (740 mg gallic acid/kg oil) and EvooB and EvooC exhibited 505 and 261 mg gallic acid/kg oil amounts of these molecules, respectively.

POV trends, expressed as normalized data, were shown in Fig. 1 for the three oils during storage and they reflected the compositional data discussed above in terms of fatty acid composition and phenolic contents. EvooA exhibited a very limited increase of POV up to 12th week of thermal stress, whereas consistent increments were registered for EvooB and EvooC (36 and 22 times the initial value, respectively). Only at the 20th week of the accelerated storage test, EvooA evidenced a high value of peroxide compounds. On the other hand, EvooB and EvooC significantly decreased in POV after 12 weeks of accelerated storage test, supposedly as a consequence of the conversion of the primary in secondary oxidation products as well as in volatile compounds [24].

DSC analysis of non-isothermal crystallization

The DSC cooling curves of EvooA and EvooB carried out at 2 °C min^{-1} for different storage times (0, 4, 12, and 20 weeks) are shown in Fig. 2, while those of EvooC are

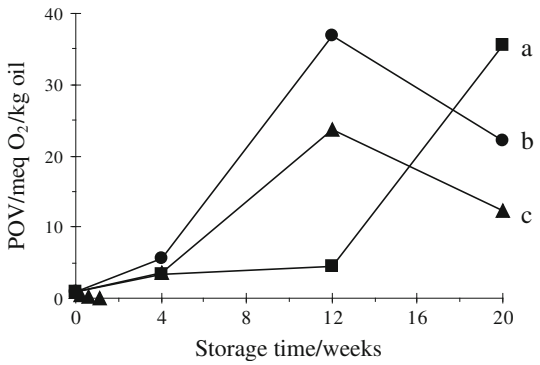

Fig. 1 Peroxide values (normalized data) of EvooA, EvooB, and EvooC at different storage times. **a** EvooA; **b** EvooB; **c** EvooC

not provided, since they are very similar to those of EvooB. The thermal behaviors of the Evoo samples not subjected to thermal treatment (0 weeks) were found to be similar to those found for other Evoo samples in previous studies [23, 25, 26]. The first sharp and symmetric exothermic DSC peak in Fig. 2a has been previously attributed to the crystallization of unsaturated triglycerides, while the second broad and asymmetric DSC peak to the fraction of more saturated triglycerides [23, 27].

The most significant difference between the two DSC curves of EvooA and EvooB is related to the shift of the second peak toward higher temperature for the latter, probably due to a more lipid saturation of this oil with respect to the other two samples, as previously reported [23, 25–27]. Another important difference is concerning the temperature range of the whole transition for samples at 0 weeks, whose values are 33.5, 38.4 and 35.4 °C for EvooA, EvooB and EvooC, respectively. The lowest value of the temperature range in EvooA can be statistically correlated to the highest content of oleic acid, as previously shown [28]. In fact, it was recently reported in the literature that this compositional characteristic may lead, during the occurrence of the transition, to a more ordered crystalline structure because of the presence of the more unsaturated triacylglycerols such as triolein [23, 25–27].

Changes of crystallization DSC profiles occurring in the Evoo samples during the period in which they were subjected to the accelerated oxidative tests confirmed what was recently found in recent studies on olive oils under comparable operative conditions [29, 30]. In particular, the comparison of DSC cooling curves of EvooB (and EvooC, even if they were not shown) with those of EvooA at higher storage times (12 and 20 weeks) seem to suggest that the extent of degradation in the formers is higher than in the latter. A further confirmation of this result is given by the fact that the more intense DSC peak at the highest storage time (20 weeks), attributed to the presence of unsaturated triacylglycerols substantially disappears in both EvooB and EvooC samples. The possible explanation of this behavior for vegetable oils was given by Tan and Che Man [31, 32], who hypothesize that, with increasing extent of thermo-oxidation, the presence of the increasing content of polar lipid molecules, which did not crystallize in the temperature range investigated, enables the decrease in the intensity of the DSC peak until its final disappearance, when the unsaturated triacylglycerols were completely transformed.

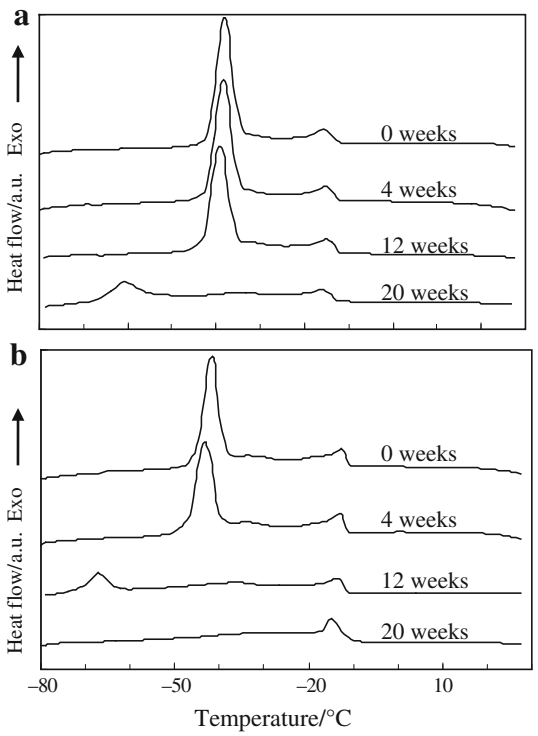

Fig. 2 DSC cooling curves at different storage times under a heating rate of 2 °C min^{-1} for: **a** EvooA; **b** EvooB

Kinetic analysis of non-isothermal crystallization

The kinetic analysis of non-isothermal crystallization of the Evoo samples tested is performed by processing only the first deconvoluted DSC peak of each curve (attributed to the crystallization of unsaturated triglycerides between −60 and −30 °C) at four cooling rates. As an example, the (not deconvoluted) DSC curves of EvooA at 1, 2, 3, and 5 °C min^{-1} in Fig. 3 showed the expected general trend as reported in the literature [33]: a shift to lower temperatures with the increase in the cooling rate. In addition, a decrease of the crystallization enthalpy (from 63.3 to 51.2 kJ mol^{-1}) with the increase of the cooling rate can be ascribed to the fact that the molecules cannot interact in an ordered way to crystallize properly. At higher cooling rate, some triglycerides contained in the Evoo samples tested crystallize into less stable form because of the higher decrease of the sample temperature, which avoid the complete crystallization of the more stable form. As expected, the behaviors shown at the highest cooling rate in the fresh samples become more evident in the samples subjected to the accelerated test as the storage time increases because of the effects produced by oxidation.

The typical time and temperature dependences of the degree of crystallinity are described in Fig. 4a, b, respectively, for fresh EvooA sample at the four different cooling rates: the higher cooling rate, the shorter crystallization time, and higher crystallization temperature. After the values of the degree of crystallinity have been obtained at each temperature and cooling rate (and obviously at each crystallization time) from the slope and intercept of each $\ln\{-\ln[1-X(t)]\}$ versus $\ln(t)$ regression line, the values of

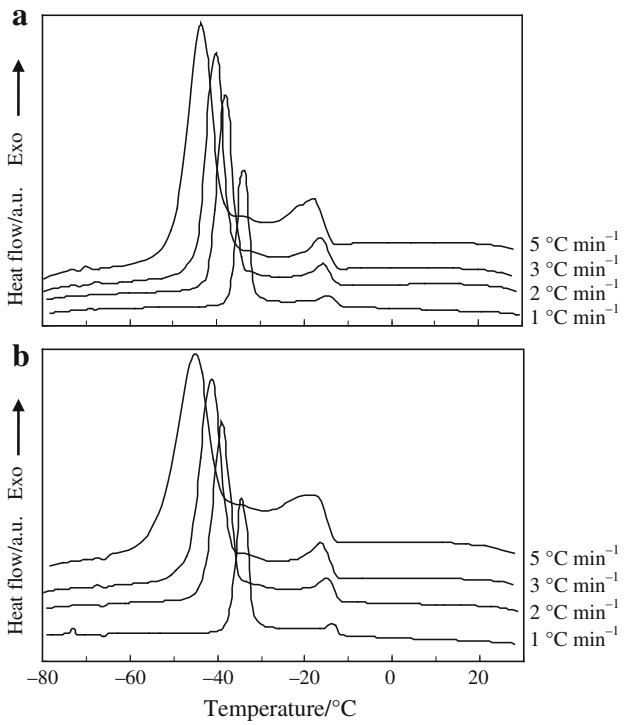

Fig. 3 DSC cooling curves of EvooA at different cooling rates at **a** 0 weeks of storage (not subjected to thermal treatment); **b** 12 weeks of storage

n and $-\ln K'$, estimated at each cooling rate and storage time, are listed in Table 1. It is worth noting that the modified Avrami approach is suitable for describing the crystallization of these samples under the experimental conditions tested, as reasonable values of n ranging from 2 to 4 are obtained, with those of fresh samples always being lower than those subjected to the accelerated oxidation test. In particular, fresh EvooA and EvooB showed values close to 3.0 (attributed to spherulitic growth from instantaneous nuclei [14, 15]), while that of EvooC is close to 2.0, thus suggesting that the nucleation should proceed via a disk-like or rod-like growth [14, 15]. Oxidized samples showed values of n slightly higher than the corresponding fresh ones without any evident correlation with the storage time. Table 1 shows that the crystallization rate constant values K', adjusted according to Jeziorny [16], increase with increase in the cooling rate. In addition, the comparison of values calculated at the same cooling rate suggests that crystallization (actually the process described by the first DSC peak) is relatively fast for fresh samples and after the first month (4 weeks). In addition, it is noteworthy that crystallization seems to occur faster for EvooC, whereas it is slower for EvooB and EvooA, overall, with an opposite trend in comparison to the phenol content. Thus, the influence of phenols on the crystallization rate cannot be excluded.

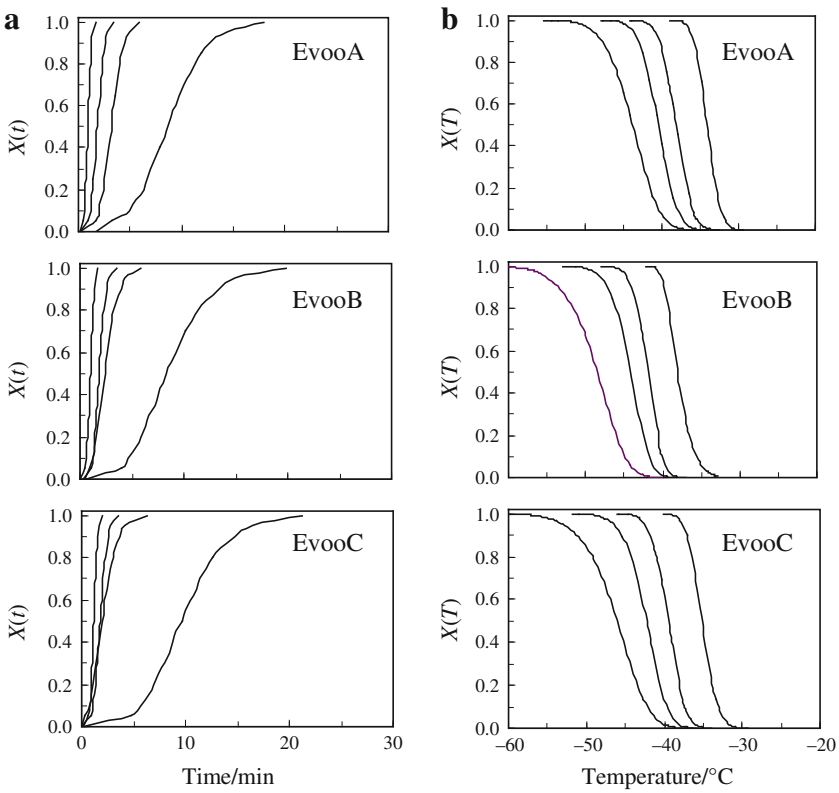

Fig. 4 Time (**a**) and Temperature (**b**) dependences of the degree of crystallinity X of fresh EvooA (0 weeks) at the four different cooling rates (1, 2, 3, and 5 °C min^{-1}, from right to left in plot **a** and from left to right in plot **b**, respectively)

The K' values seem to indicate that the crystallization rate decreases with increasing the storage time for all the samples. This fact is particularly evident in EvooC, where the highest values of $-\ln K'$ are found in Table 1 at 12 and 20 weeks at a cooling rate of 1 °C min^{-1} (when the process occurs at the slowest rate and reaches its completeness with the largest crystallization time). This behavior can be explained by the presence of lipid oxidation products (and products of lipid hydrolysis such as mono and diacylglycerols) that can be intercalated into the

Table 1 Kinetic parameters of non-isothermal crystallization (first DSC peak) for Evoo samples at the four different storage times (0, 4, 12, and 20 weeks) according to the Avrami approach [14, 15]

β/°C min^{-1}	n				$-\ln K'^{a}$				$t_{1/2}$/min			
	0	4	12	20	0	4	12	20	0	4	12	20
EvooA												
1	3.2	4.0	3.4	3.9	8.0	9.9	8.7	10.0	8.7	10.5	12.9	14.7
2	2.8	3.7	3.7	4.0	1.6	2.0	2.3	2.5	3.2	3.5	3.7	4.1
3	2.9	3.3	3.4	3.8	0.7	0.9	1.0	1.1	1.8	1.9	2.7	3.3
5	3.2	3.6	3.8	3.7	0.02	0.04	0.1	0.2	0.9	0.9	1.4	1.6
EvooB												
1	2.7	3.8	2.9	2.9	6.1	7.4	7.8	8.2	8.4	8.8	12.6	14.5
2	3.2	3.0	3.1	3.0	1.6	2.1	2.4	2.6	2.4	3.6	3.9	4.4
3	3.4	2.5	3.5	2.9	0.8	1.1	1.0	1.1	1.8	3.1	1.9	2.4
5	2.2	3.1	2.3	3.1	0.07	0.6	0.6	0.7	1.1	2.4	1.5	1.9
EvooC												
1	1.7	2.8	3.6	2.8	4.3	6.9	14.6	18.1	9.6	10.3	12.9	14.9
2	1.7	2.6	2.6	2.9	0.8	1.7	1.9	2.3	2.0	3.6	3.7	4.4
3	2.2	2.7	3.3	3.1	0.5	0.7	1.2	1.4	1.8	1.9	2.7	3.0
5	2.8	3.2	3.6	3.0	0.2	0.2	0.3	0.4	1.2	1.1	1.4	1.7

Relative standard deviation (RSD) of all data is always less than 5%

[a] Units of K' depends on the value of n estimated

Table 2 Kinetic parameters of non-isothermal crystallization (first DSC peak) for Evoo samples at the four different storage times (0, 4, 12, and 20 weeks) for different degrees of crystallinity, according to the Liu-Mo approach [19]

$X(T)$	$F(T)$				b			
	0	4	12	20	0	4	12	20
EvooA								
0.2	2.1	2.1	2.1	2.2	1.2	1.1	1.1	1.1
0.4	2.0	2.0	2.0	2.1	1.2	1.1	1.1	1.1
0.6	1.9	1.9	2.0	2.0	1.2	1.1	1.1	1.1
0.8	1.8	1.8	1.8	1.9	1.2	1.1	1.1	1.0
EvooB								
0.2	2.1	2.2	3.2	3.4	1.2	1.1	1.9	2.1
0.4	2.0	2.1	2.8	3.0	1.3	1.2	1.8	2.0
0.6	1.9	2.1	2.5	2.6	1.3	1.2	1.7	1.9
0.8	1.7	1.9	2.2	2.5	1.3	1.2	1.5	1.9
EvooC								
0.2	2.1	2.2	2.4	2.6	1.2	1.2	1.3	1.5
0.4	2.0	2.1	2.2	2.4	1.2	1.2	1.2	1.4
0.6	1.8	2.0	2.1	2.3	1.2	1.2	1.2	1.3
0.8	1.7	1.9	2.0	2.2	1.1	1.2	1.2	1.3

Relative standard deviation (RSD) of all data is always less than 3% and $r^2 > 0.993$ (4 regression data points)

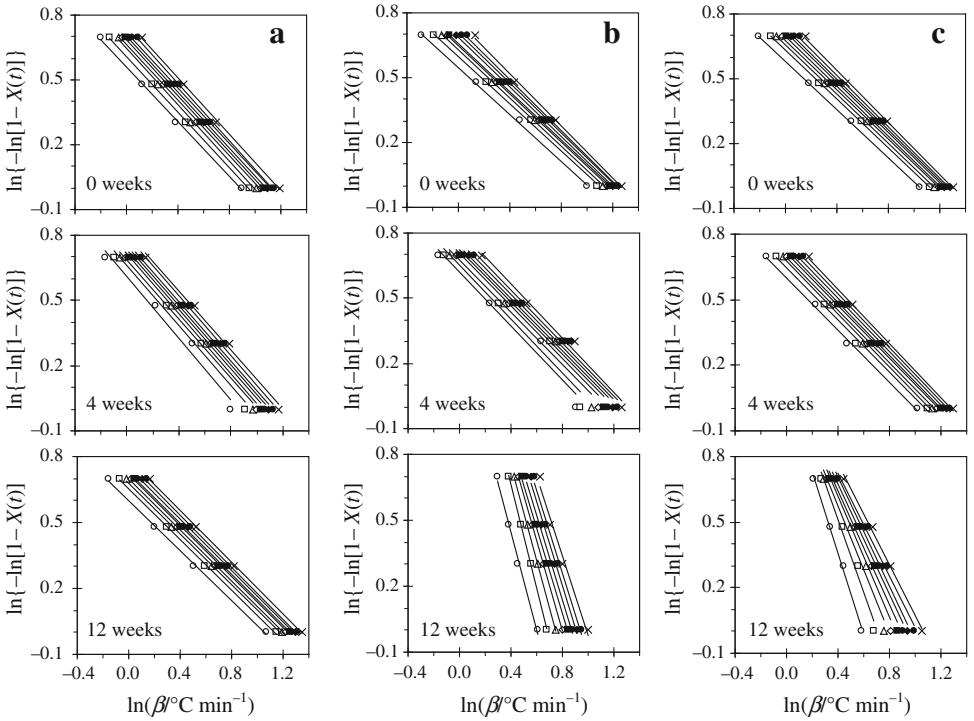

Fig. 5 Ozawa plot of the non-isothermal crystallization at 0, 4, and 12 weeks of storage for each of the nine regression lines at constant degree of crystallinity ($r^2 > 0.990$, 4 regression data points) **a** EvooA; **b** EvooB; **c** EvooC

molecules of triglycerides, causing an increase of the disorder, as previously reported [34].

The values of the half-time of non-isothermal crystallization, $t_{1/2}$, estimated from Fig. 4a at $X(t) = 0.5$, are summarized in Table 1. As expected, these values decrease with increasing values of the cooling rate and decreasing values of the storage time, the lowest values being those calculated for fresh samples. Only slight differences can be found among values derived by different Evoos at the same cooling rate and storage condition.

The analysis of results derived by the Avrami approach and its Jeziorny modification [16] must be completed by combining Avrami and Ozawa methods, using Eqs. 4 and 5. The results of the Ozawa method are displayed in Fig. 5. The values of m derived by the slope values, being equal to $-m$ according to Eq. (3), were found to be in agreement (sometimes slightly lower) with those calculated using the Avrami method. The values of $F(T)$ and b, determined from the slope and intercept of each regression line obtained by plotting $\ln\beta$ versus $\ln t$ at fixed degrees of crystallinity (Eq. 5), are reported in Table 2. At the same degree of crystallinity, the values of both $F(t)$ and b showed no significant differences with increasing values of the storage time, except for EvooB and EvooC at higher storage times (12 and 20 weeks), where higher values were found, probably caused by the presence of a higher content of lipid oxidation products. At the same storage condition (fresh samples or samples at the same storage time), a decreasing trend was observed for the values of $F(t)$ with increasing values of the degree of crystallinity, thus demonstrating that a lower cooling rate should be required to obtain a higher degree of crystallinity in the same crystallization time. The constancy of values of b, very close to unity (with the above-mentioned exceptions) confirms the assessment of mechanisms of crystal growth made on the basis of the Avrami method only.

Conclusions

Kinetic parameters of non-isothermal crystallization were calculated for the three Evoo samples tested, which have different total phenol contents and fatty acid compositions, according to both the modified Avrami and Ozawa methods. The results derived by the modified Avrami method were reasonable ($n \leq 4$) and show that crystallization rate is influenced by the total phenol contents and fatty acid compositions mainly in oxidized samples: this process is relatively fast in fresh samples, and after the first 4 weeks, it occurs at slower rate in EvooB and EvooC, where a higher extent of oxidation was found. Anyway, an influence of phenols on the crystallization rate of fresh samples cannot be excluded and need to be further explored.

Finally, results derived by the Ozawa method confirm those obtained with the modified Avrami method (b close to 1), thus demonstrating the suitability of a non-isothermal approach to describe the crystallization of Evoos under conditions that mimic those commonly occur during storage.

Acknowledgements The authors gratefully acknowledge the assistance of Dr. Alessandra Bendini (university of Bologna) for the treatment of chemical data.

References

1. Frankel EN. Chemistry of extra virgin olive oil: adulteration, oxidative stability, and antioxidants. J Agric Food Chem. 2010; 58:5991–6006.
2. Lercker G, Frega N, Bocci F, Servidio G. Veiled extra-virgin olive oils: dispersion response related to oil quality. J Am Oil Chem Soc. 1994;71:657–8.
3. Calligaris S, Sovrano S, Manzocco L, Vicoli MC. Influence of crystallization on the oxidative stability of extra virgin olive oil. J Agric Food Chem. 2006;54:529–35.
4. Hammami A, Mehrota AK. Non-isothermal crystallization kinetics of n-paraffins with chain lengths between thirty and fifty. Thermochim Acta. 1992;211:137–53.
5. Kaygili O, Yavuz H. The effects of gamma irradiation on non-isothermal crystallization kinetics and microhardness of the Li_2O–Al_2O_3–SiO_2 glass-ceramic. J Therm Anal Calorim. 2010;102: 681–4.
6. Păcurariu C, Lazău RI, Lazău I, Ianoş R, Tiţa B. Non-isothermal crystallization kinetics of some basaltic glass-ceramic containing CaF_2 as nucleating agent. J Therm Anal Calorim. 2009;97: 507–13.
7. Păcurariu C, Lazău RI, Lazău I, Tiţa B, Dumitrel A. Non-isothermal crystallization kinetics of some aventurine decorative glaze. J Therm Anal Calorim. 2011;105:435–41.
8. Papageorgiou GZ, Achilias DS, Bikiaris DN, Karayannidis GP. Isothermal and non-isothermal crystallization kinetics of branched and partially crosslinked PET DSC study. J Therm Anal Calorim. 2006;84:85–9.
9. Zhang Z, Chen C, Wang C, Guo J, Mai K. Nonisothermal crystallization kinetics of isotactic polypropylene nucleated with a novel supported β-nucleating agent. J Therm Anal Calorim. 2011; 103:311–8.
10. Ma W, Wang X, Zhang J. Crystallization kinetics of poly(vinylidene fluoride/MMT, SiO_2, $CaCO_3$, or PTFE nanocomposite by differential scanning calorimeter. J Therm Anal Calorim. 2011;103:319–27.
11. Vyazovkin S, Stone J, Sbirrazzuoli N. Hoffmann-Lauritzen parameters for non-isothermal crystallization of poly(ethylene terephtalate) and poly(ethylene oxide) melts. J Therm Anal Calorim. 2005;80:177–80.
12. Di Lorenzo ML, Silvestre C. Non-isothermal crystallization kinetics of polymers. Prog Polym Sci. 1999;24:917–50.
13. Martini S, Herrera ML, Hartel RW. Effect of cooling rate on crystallization behavior of milk fat fraction/sunflower oil blends. J Am Oil Chem Soc. 2002;79:1055–62.
14. Avrami M. Kinetic of phase change. I. General theory. J Chem Phys. 1939;7:1103–12.
15. Avrami M. Kinetic of phase change. II. Transformation-time relations for random distribution of nuclei. J Chem Phys. 1940; 8:212–24.
16. Jeziorny A. Parameters characterizing the kinetics of the non-isothermal crystallization of poly(ethylene terephtalate) determined by d.s.c. Polymer. 1978;19:1142–4.
17. Ozawa T. Kinetics of non-isothermal crystallization. Polymer. 1971;12:150–8.
18. López LC, Wilkes GL. Non-isothermal crystallization kinetics of poly(*p*-phenylene sulphide). Polymer. 1989;30:882–7.
19. Liu TX, Mo ZS, Wang SG, Zhang HF. Nonisothermal melt and cold crystallization kinetics of poly(aryl ether ether ketone ketone). Polym Eng Sci. 1997;37:568–75.
20. Bendini A, Cerretani L, Vecchi S, Carrasco-Pancorbo A, Lercker G. Protective effects of extra virgin olive oil phenolics on oxidative stability in the presence or absence of copper ions. J Agric Food Chem. 2006;54:4880–7.
21. Bonoli M, Bendini A, Cerretani L, Gallina Toschi T, Lercker G. Qualitative and semiquantitative analysis of phenolic compounds in extra virgin olive oils as a function of the ripening degree of olive fruits by different analytical techniques. J Agric Food Chem. 2004;52:7026–32.
22. European Community (EC). Commission Regulation 1513/2001 of 23 July 2001 amending Regulations No 136/66/EEC and (EC) No 1638/98 as regards the extension of the period of validity of the aid scheme and the quality strategy for olive oil. Off J Eur Commun. L 1991;248:1−83.
23. Chiavaro E, Vittadini E, Rodriguez-Estrada MT, Cerretani L, Bonoli M, Bendini A, Lercker G. Monovarietal extra virgin olive oils: correlation between thermal properties and chemical composition. J Agric Food Chem. 2007;55:10779–86.
24. Morales MT, Rios JJ, Aparicio R. Changes in the volatile composition of virgin olive oil during oxidation: flavors and off-flavors. J Agric Food Chem. 1997;45:2666–73.
25. Chiavaro E, Vittadini E, Rodriguez-Estrada MT, Cerretani L, Bendini A. Differential scanning calorimetry application to the detection of refined hazelnut oil in extra virgin olive oil. Food Chem. 2008;110:248–56.
26. Chiavaro E, Rodriguez-Estrada MT, Barnaba C, Vittadini E, Cerretani L, Bendini A. Differential scanning calorimetry: a potential too for discrimination of olive oil commercial categories. Anal Chim Acta. 2008;625:215–26.
27. Tan CP, Che Man YB. Differential scanning calorimetry analysis of edible oils: comparison of thermal properties and chemical composition. J Am Oil Chem Soc. 2000;77:143–5.
28. Chiavaro E, Rodriguez-Estrada MT, Bendini A, Cerretani L. Correlation between thermal properties and chemical composition of Italian extra virgin olive oils. Eur J Lipid Sci Technol. 2010;112:580–92.
29. Chiavaro E, Mahesar S, Bendini A, Foroni E, Valli E, Cerretani L. DSC evaluation of olive oil during an accelerated oxidation. It J Food Sci. 2011;23:164–72.
30. Chiavaro E, Rodriguez-Estrada MT, Bendini A, Rinaldi M, Cerretani L. DSC thermal properties and oxidative stability indices of microwave heated extra virgin olive oils. J Sci Food Agric. 2010;91:198–206.
31. Tan CP, Che Man YB. Quantitative differential scanning calorimetry analysis for determining total polar compounds in heated oils. J Am Oil Chem Soc. 1999;76:1047–57.
32. Tan CP, Che Man YB. Differential scanning calorimetry analysis for monitoring the oxidation of heated oils. Food Chem. 1999;67:177–84.
33. Tan CP, Che Man YB. Comparative differential scanning calorimetric analysis of vegetable oils: I Effect of heating rate variation. Phytochem Anal. 2002;13:129–41.
34. Che Man YB, Swe PZ. Thermal analysis of failed-batch palm oil by differential scanning calorimetry. J Am Oil Chem Soc. 1995;72: 1529–32.